# INFLUENCE OF ADSORBATES AND SURFACE COMPOUNDS ON THE FIELD EMISSION OF NIOBIUM

T. HABERMANN, A. GÖHL, D. NAU, G. MÜLLER, H. PIEL, M. WEDEL

Fachbereich Physik, Bergische Universität Wuppertal, Gaußstr. 20, D-42097 Wuppertal, Germany

In order to achieve a deeper insight into the phenomena observed at 'parasitic' field emitters, the 'intrinsic' field emission of typical, flat niobium surfaces was systematically investigated. A dc Field Emission Scanning Microscope was employed to measure locally (several $\mu m^2$) the onset field strength and Fowler Nordheim parameters on wet-chemically prepared, ion-etched, and UHV heat-treated samples. The averaged onset field strengths were determined for different treatments on four samples to be between 0.9 GV/m and 2.3 GV/m. Considering the residual surface roughness this corresponds very well with the 2.2 GV/m predicted by the Fowler Nordheim theory for the numerically calculated fields in the experimental setup. Surface purity and chemical composition of the investigated areas were *in situ* analyzed by Scanning Electron Microscopy and Auger Electron Spectroscopy. We have found a correlation between the Fowler Nordheim parameter $\beta_{FN}$ (field enhancement factor) and $S_{FN}$ (effective emitting area) of 'parasitic' emitters. This correlation as well as strong variation in $S_{FN}$, and unrealistically high $S_{FN}$ were empirically described and found to strongly depend on adsorbates. The measurements on the 'intrinsic' emission, where the chemical surface composition is well known and the residual surface roughness is easier to estimate, confirmed these findings. UHV heat treatments at temperatures between 200°C and 800°C are known to activate particles on the surface to strong field emission. Our observations indicate a dependence of this activation on the conduction properties of the particle or the interface. Therefore the role of the insulating $Nb_2O_5$ layer, present on niobium after wet surface preparation or air exposure, and of niobium carbides and niobium sulfides will be discussed.

## 1. INTRODUCTION

The quest for high gradients in superconducting rf accelerating cavities suffers from two main limitations: defect-induced thermal breakdown, and 'parasitic' field emission (FE) due to local defects or particulate contamination. [1] In the past several studies dealt with the latter in order to improve the performance of the cavities by better surface preparation [2] as well as to progress in the understanding of the emission mechanisms. At first one suspected a simple geometric field enhancement due to metallic protrusions as the reason for the strong electron emission. [3] Since such shapes expected from the FE analysis were not found [4] and several observed phenomena could not be explained, more complex models connected with the presence of insulators and metal insulator metal structures were developed, but not systematically correlated to the 'parasitic' FE. [5, 6] Alternatively, a 'protrusion-on-protrusion' model considering an additional geometric field enhancement by the micro-roughness of electron emitting particles [7] predicted the required geometric field enhancement for the observed FE. The comparison between in this way geometrically deduced FE parameters and measured parameters obtained from Fowler Nordheim (FN) analysis of emitters on a broad area Nb cathode showed an astonishingly good agreement. The FE behavior after deposition of a thin gold layer onto these emitters confirmed a mainly geometrically dominated emission mechanism. Additionally, the influence of adsorbates and surface compounds on the

electron emission became evident by the fluctuation of the FE parameters of individual emitters. [8, 9] It is well known that Nb and other metals after wet surface preparation are covered by oxides and adsorbates [10], and their effect on the FE behavior is reported in many studies. [11-14]
In this work, local measurements of the 'intrinsic' FE behavior of broad area Nb cathodes by means of a Field Emission Scanning Microscope (FESM) are presented. Several samples were analyzed after different surface treatments, e.g. ion bombardment and heating. The flat Nb surface allows a better estimation of geometrical effects and its chemical composition is well known. Therefore, this study describes the influence of adsorbates and surface compounds on the FE and leads also to a progress in the description of such phenomena observed at 'parasitic' field emitters.

## 2. EXPERIMENTAL SETUP, METHODS, AND SAMPLE PREPARATION

Two ultra high vacuum (UHV) chambers connected by a gate valve contain the FESM combined with a commercial surface analysis equipment, and an *in situ* electron beam furnace for heat treatments (HT) of samples up to 2000°C. With this system the samples are introduced without breaking the vacuum of the analysis chamber. The FESM consists of a computer controlled, mechanical xyz-sample-manipulator with a step width of 63.5 nm. A fast regulated high voltage can be applied to fixed tungsten anodes of different, optional size. This allows both measurement of the FE distribution of cm²-sized flat samples by scanning, and localization and analysis of single emitters with µm resolution without destroying them by high currents. At present this system is supplemented by a Piezo-driven translator system for enhanced resolution. Morphology and chemical composition can be *in situ* analyzed at any site by scanning electron microscopy (SEM) and Auger electron spectroscopy (AES). Furthermore it is possible to locally remove material from the surface by means of a micro-focus Ar-ion-gun (EX050S, Fisons Instruments). A more detailed description of the system and the procedure for analysis of the 'parasitic' FE is given elsewhere. [15-17]
The measurement of the 'intrinsic' FE was generally carried out as follows. A micro-tip anode (radius of curvature here typically 5 µm) was located over any arbitrary site of the sample. SEM inspection guaranteed analysis of an uncontaminated site. Then the voltage U was increased and the electrode distance z decreased until a FE current I of 0.5 nA was reached, and the onset field strength $E_{on}$ = E(0.5 nA) was determined by plotting U vs. z. The FN parameter $\beta_{FN}$ as the 'field enhancement factor' and $S_{FN}$ as the 'effective emitting area' were obtained from recording the $\ln(I/E^2)$ vs. 1/E curve between 0.5 nA and 10 nA, assuming a work function of 4.0 eV and without image force correction. In this way the data of about 30 sites were taken to get average FE parameters of each sample after each surface treatment. In total four samples were examined. Two samples (D1, D3) were made from Heraeus Nb with an original residual resistance ratio (RRR) of 300, and a grain size in the order of mm after UHV HT (1400°C, 60 min). The samples PK5 and PK9 were fabricated from Wah Chang Nb sheet (originally RRR ≈ 250) with a grain size of about 10 µm. At the beginning of these experiments the four samples obtained a wet surface preparation. The surface desorption by Ar-sputtering was carried out with two different settings: scanned beam with an accelerating voltage of 5 kV (1 kV), $Ar^+$ - $Ar^{+++}$ ($Ar^+$), a sputter rate of 4.1 nm/min (0.33 nm/min), and a total removal of 250 nm (15 nm). Comparative studies on one sample resulted in the same FE behavior for these different settings. The pressure level for the measurements was $1 \cdot 10^{-9}$ mbar. After sputter desorption it took one hour to detect again O or C by AES. Hence the values for the category 'pure Nb' were taken within the first 45 min after sputtering, 're-adsorbed Nb' describes the sputtered surface after several days in the UHV, and 're-oxidized' after several days in air. The samples D3 and PK5 were additionally heat treated at 400°C for 60 min, the heating of sample PK5 at 1400°C took 30 min.

## 3. RESULTS AND DISCUSSION

In the first part of this chapter important results on the 'parasitic' FE are presented, while the findings regarding the 'intrinsic' electron emission are described in the second part. Their impact on the explanation of the 'parasitic' FE will be also discussed.

### 3.1 'Parasitic' Field Emission

In many investigations heating at temperatures above 1200°C has been reported as a powerful means to reduce significantly the FE of a Nb sample. [2, 15, 18, 19] As shown by AES, a diffusion of O and therefore a decrease of the O content at the surface can be generally observed in the temperature range around 1400°C. Comparative SEM analysis of 14 emitting particles which were deactivated by 30 min at 1400°C showed that two particles had disappeared, three particles were still there but in a different appearance, while 64% of these particles did not reveal a visible change of their morphology. [9]

On the other hand, FE-activation of non-emitting particles on differently prepared Nb surfaces was observed after *in situ* HT between 200°C and 800°C. [2, 18, 19] At such temperatures diffusion phenomena of light atoms in the Nb as well as adsorption, desorption, and chemisorption of adsorbates take place. As reported in ref. 17, we observed a dependence of this activation process on the purity of the cathode material, i.e. the diffusion of impurities is responsible for or at least affects the activation. Chemical surface analysis by AES showed after this kind of HT besides the O reduction a significant S content or an enhanced (carbidic) C signal. [9] The occurrence of S on the surface can be ascribed to the segregation from the bulk. It seems that this behavior strongly depends on the material, i.e. on the supplier of the Nb. In contrast, the amount of the Nb carbides on the surface rather depends on the vacuum conditions during the HT, like the partial pressure of carbon oxides and hydrocarbons. Comparison of local AES of 11 activated emitting sites with integral spectra of the samples revealed either an enhanced sulfur or an enhanced carbon content (see Fig. 1). It is known from literature [20, 21] that at temperatures between 200°C and 800°C there exist orthorhombic phases of $Nb_2C$ and $NbS_2$, which have layered, anisotropic properties. Similar FE behavior as well as similar structural properties of $MoS_2$ and graphite were reported in ref. 22. At temperatures above 1200°C $Nb_2C$ and $NbS_2$ change to their hexagonal phase, dissolve and/or evaporate. The question whether the formation of certain phases of $Nb_2C$ or $NbS_2$ is related to the activation process will be discussed later.

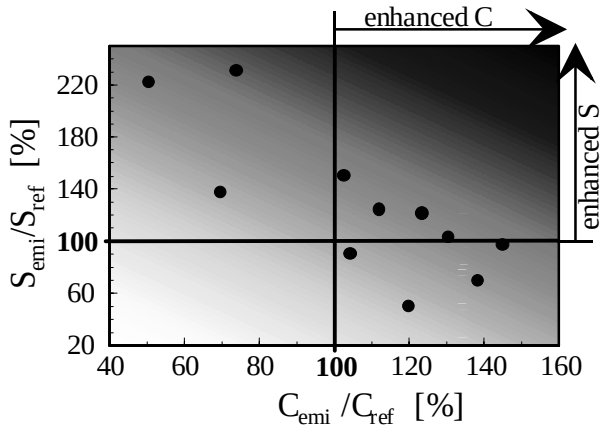


FIGURE 1: Relative carbon and sulfur signal at FE-activated (400°C) emission sites compared to the integral AES analysis of the sample. [9]

Another point, that has to be discussed, is the role of the surface oxides. Neither our studies [2] nor experiments performed in other laboratories [11, 22] detected any influence of a (thick) insulating $Nb_2O_5$ layer on the FE behavior of particles. The layer decreases or disappears while heating at 200°C to 800°C ('activation') as well as at 1400°C ('deactivation'). We never observed, however, FE from particles, that charged up in the SEM, i.e. insulating or electrical isolated particles. By SEM analysis of particles before and after HT activation we saw several times charging before, but never after activation. This indicates that the conducting state of the particles or of the contact, influenced

by diffusion and phase transition, may be important for both the activation and the deactivation phenomena. Further experiments have to clarify this point, e.g. by tracing back the history of an activated particle by means of video scans combined with SEM observation before HT and after HT, but before the FE measurement.

Several phenomena of our previous studies can be ascribed to the influence of adsorbates. E.g. we observed that the amount of I vs. E curves with unstable behavior is lower for *in situ* heat treated than for wet prepared Nb samples. [16] FN analysis of several hundreds of emitting sites showed a correlation between the parameters $\beta_{FN}$ and $S_{FN}$, which are in principle independent. [16, 17] At high $\beta_{FN}$ small $S_{FN}$-values were preferably observed and vice versa. Furthermore a considerable fraction of the measured $S_{FN}$ is unrealistically high and the $S_{FN}$-values are widely spreaded. Examples from other laboratories, where significant changes in the $S_{FN}$ due to adsorbates were observed, can be found in refs. 13 and 23. As demonstrated by a impressive example, these phenomena, namely unrealistic and widely distributed $S_{FN}$, and a correlation between $\beta_{FN}$ and $S_{FN}$, can even be observed at a single, unstable emission site. [9] At emitter 'H3#206' we repeatedly performed FN analysis with widely varying results. It can be seen from Fig. 2 that the changes in the FN parameters took place along a certain curve. As indicated by the numbers, we can not ascribe this behavior to a certain conditioning like e.g. geometric blunting due to the current flow, because the changes do not go only in one direction. With this example we can empirically describe the additional influence of adsorbates on the FE of geometric field enhancing particles. Assuming that the geometrical field enhancement factor $\beta_{geo}$ is changed by a factor $c = \beta_{FN}/\beta_{geo}$, the S-parameter is changed in a correlated way: $S_{FN} = m(c) \cdot S_{geo}$. If we assume realistic values $\beta_{geo} = 82$ and $S_{geo} = 1 \cdot 10^{-12}$ cm², which fulfill the boundary condition $S_{FN} = S_{geo}$ for $c = 1$, we can fit the data of H3#206 and receive an empirical function to describe the changes of the FN parameters due to adsorbates:

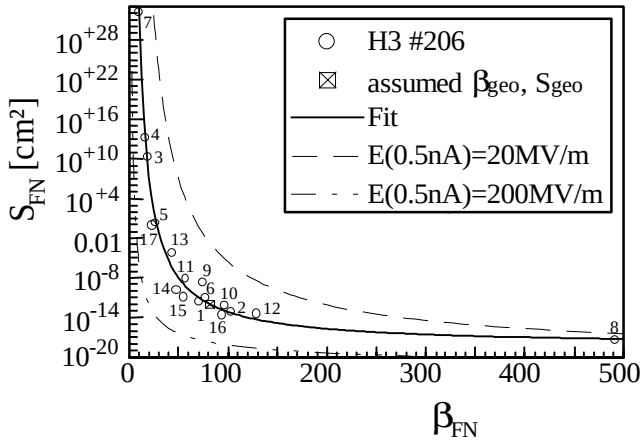


FIGURE 2: Varying emission behavior of a repeatedly measured, unstable 'parasitic' field emitter. The solid line represents the function obtained from these data under the assumption of realistic values for $\beta_{geo}$ and $S_{geo}$. [9]

$$S_{FN} = S_{geo} \cdot 5.58 \cdot 10^{-7} \cdot \exp(14.40 \cdot \beta_{geo} / \beta_{FN})$$

### 3.2 'Intrinsic' Field Emission

Different emitting particles usually reveal a strong variation of their geometric conditions and their chemical composition. Experimentally these properties of an emitter are difficult to identify. Therefore, an investigation of the 'intrinsic' FE properties of differently prepared broad area Nb surfaces was performed. Under these conditions 'parasitic' FE can be avoided by SEM inspection, the chemical composition is analyzed by AES, and the geometric field enhancement due to the residual roughness can be estimated to be in general between 1 and 3. The chemical analysis of sample PK5 is shown in Fig. 3. The spectra represent the typical conditions of a Nb surface after wet surface preparation, oxide removal by ion sputtering, 're-adsorption', and renewed oxidization by air exposure. In general the oxygen disappears from the surface by heating, the O peak after 1400°C is

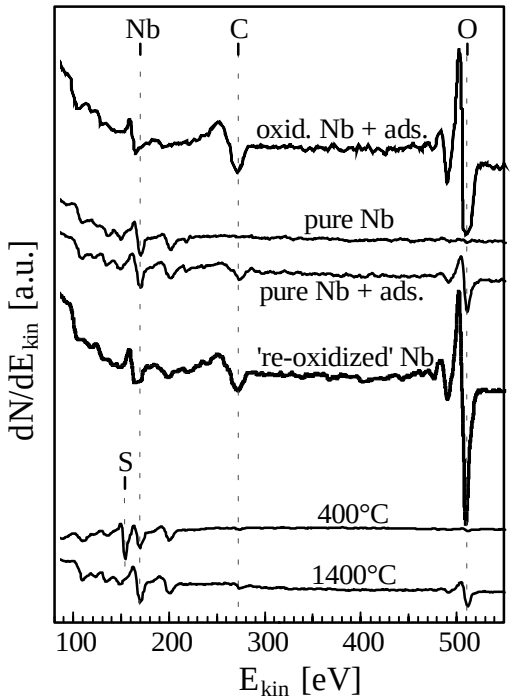


FIGURE 3: AES on sample PK5 after the different surface treatments. The main Nb peak at 167 eV is in case of oxidized Nb ($Nb_2O_5$) slightly shifted towards smaller energies.

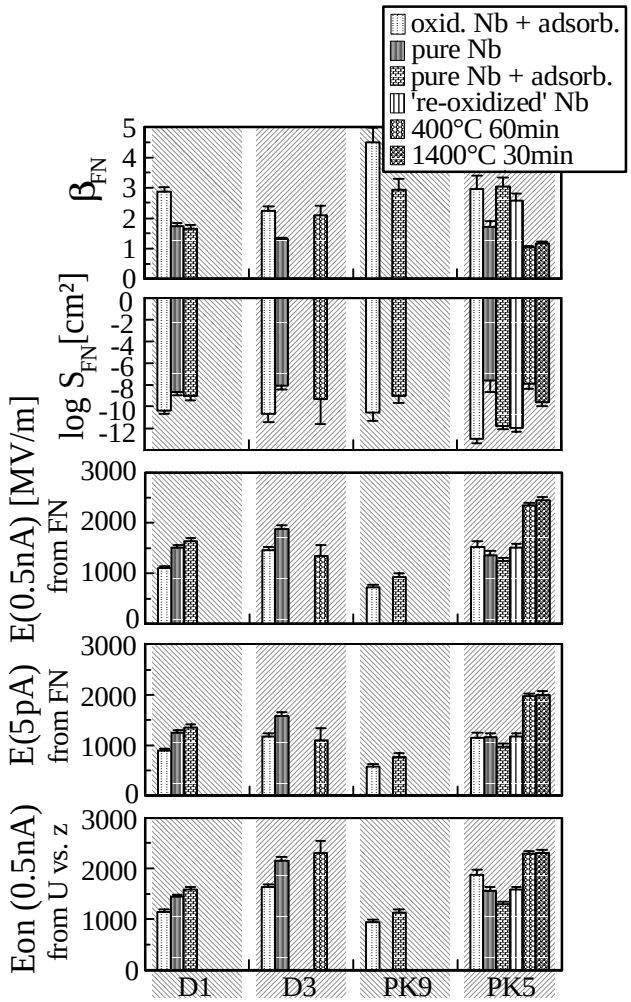


FIGURE 4: Averaged 'intrinsic' FE parameters (including their statistical error) of four Nb samples after different surface treatments.

due to a delay between the HT and the AES. The development of the other foreign elements detected here strongly depends on the cathode material. We see from the spectra of PK5 a reduction of the C content due to the HT, and a strong S-signal after 400°C. At sample D3 the C-signal after 400°C was slightly higher with a more carbidic peak shape. No segregation of S was detected at D3.
From the average FN parameters of each sample in Fig. 4 it can be seen that the adsorbate and oxide removal by Ar-sputtering led to a decrease in $\beta_{FN}$ and to an increase in $S_{FN}$. This corresponds to a smoothening of the surface roughness, but this is not the whole story since we observe again an increase in $\beta_{FN}$ and a decrease in $S_{FN}$ after air exposure ('re-oxidized'). A Nb surface after wet surface preparation is covered by a monolayer NbO, by about 6 nm $Nb_2O_5$, and by adsorbates like carbon oxides and carbon hydrates. This, of course, changes the electronic properties (e.g. work function) and therefore the FE behavior, since $Nb_2O_5$ is known as an insulator. The oxidation of the surface, i.e. the formation of $Nb_2O_5$, can additionally lead to geometric changes due to a serrating growth of the oxide into the bulk. [10] The influence of the adsorbates is not plain to see. At sample D1 the FN parameters of the pure Nb with and without adsorbates are very similar, while at PK5 the surface with adsorbates behaves similar before and after oxidization. At sample PK9, where no measurements on the pure Nb were performed, the FN parameter of the adsorbate-covered Nb surface are different from the values of the oxidized, adsorbate-covered surface. Probably PK9 behaves qualitatively similar as D1.

The effect of these different surface conditions on the 'intrinsic' onset field strength is summarized in Fig. 4. The bottom diagram was obtained from the slope of the U vs. z plot at I = 0.5 nA. This result agrees very well with E(0.5 nA), which was calculated from the $\beta_{FN}$ and $S_{FN}$ using the FN equation. By the values for E(5 pA) it becomes obvious how the FN parameters influence the FE at different current levels. By means of numerical calculations the absolute field levels can be compared with the theory. The field along a flat metal surface 1 µm below an anode with 5 µm radius of curvature at a potential of 1 V was used to calculate the relative lateral FE current (see Fig. 5). By integration of the current the effective emitting surface $S_{geo}$ is obtained. The maximum field E(r = 0) applied over $S_{geo}$ results in the same total current as the 'real' condition. For this configuration the electric field, which is necessary to get a FE current of 0.5 nA, is 2200 MV/m. This is in good agreement with the measured values since a residual surface roughness has to be taken into account.

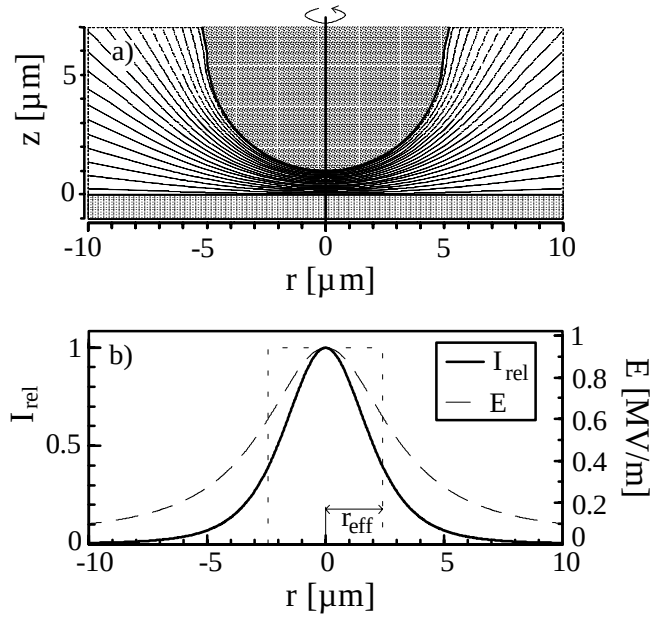


FIGURE 5: Numerical calculations by means of the program code MAFIA [24] for simulation of a microtip anode (radius of curvature: 5 µm) at a distance of 1 µm above a flat metal surface. a) Lines of constant potential. b) Electric field strength at the cathode surface after application of 1 V to the anode (— — —) and relative current (————) in lateral direction, calculated by means of the FN equation. The dotted line (- - - - - -) demonstrates an equivalent emitter with constant field strength and constant current over the effective emitting surface $S_{geo} = \pi \cdot r_{eff}^2$.

Heating of two Nb samples at 400°C (D3 and PK5) did not enhance the 'intrinsic' FE. From Fig. 4 it can be seen that at both samples $E_{on}$ was higher after the HT. Therefore, an activation process due to an enhancement of the 'intrinsic' FE on field enhancing particles by the formation of certain phases of Nb carbides or Nb sulfides can be excluded. Furthermore a HT of PK5 at 1400°C didn't change the 'intrinsic' FE behavior anymore. The presence of sulfur on the surface after the first HT did not affect the FE at all. The activation of particles by 'low temperature' HT may be connected to the decreasing oxide layer, i.e. the electric contact of conducting particles to the substrate. After getting contact a particle could emit due to geometric field enhancement. The deactivation at higher temperatures may be due melting and evaporation of material, but also due to smoothening of small sub-structures on particles. These assumptions are supported by the previous results on deactivated emitters that were analyzed before and after the HT. A question mark, however, remains for the activation of particles on a sample, that was heated at 1400°C before. We never observed a deactivated emitter to be activated again. [18] Are there still particles left, which were not yet contacted after the 1400°C? In this case the deactivation has to be connected to the status of the contact: once a particle gets in electrical contact the deactivation has to take place immediately, otherwise also HT at 1400°C should lead to an activation. Prior heating at 1400°C for several hours resulted in a lower density of activated emitters. [9] Another possibility for activation and deactivation is a phase transition in the particle, e.g. from an insulating to a conducting state.

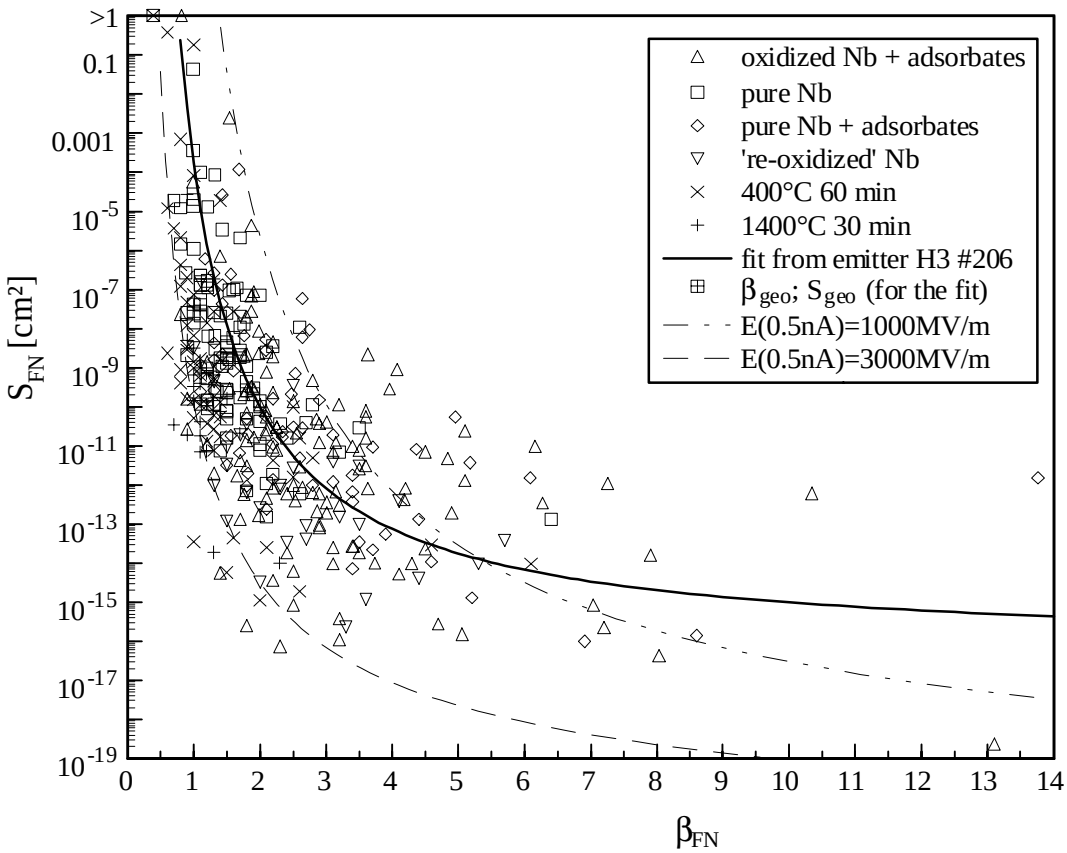


FIGURE 6: Plot of the 'intrinsic' FN parameter $S_{FN}$ vs. $\beta_{FN}$ from individual emission sites of four Nb samples after different surface treatments. The solid line shows the empirical formula for the influence of adsorbates on the FE assuming a realistic field enhancement factor $\beta_{geo} = 2$ and effective emitting area $S_{geo} = 1 \cdot 10^{-10}$ cm².

The 'intrinsic' FN parameters of the individual analyzed sites of all samples, as plotted in Fig. 6, show a similar correlation as already observed at the 'parasitic' field emitters. In a narrow range we expect such a behavior due to geometric effects. Small structures on the surface lead locally to a slight geometric field enhancement, i.e. to higher $\beta_{FN}$ and smaller $S_{FN}$. This alone, however, can not explain the observed range of the FN parameters, especially unrealistically high values of $S_{FN}$. There is no doubt that for the sputtered Nb surface we get a mainly 'metallic' emission according to the FN theory. But also in this case a few unrealistically high $S_{FN}$ were measured. Obviously already the first adsorbates, that arrive at the surface, can change the emission properties. It was shown e.g. in ref. 25 that one single Sr atom on a W tip enhanced the FE current by two orders of magnitude. Because of the good agreement to theory and the similar behavior as for the 'pure Nb', one can assume for the heat treated, oxidized or adsorbed surfaces also a mainly 'metallic' FE. The superimposed influence of adsorbates leads to the $\beta_{FN}$-$S_{FN}$-correlation, which includes the wide spread of $S_{FN}$, especially towards the high values. In Fig. 6 also the empirical description obtained from emitter H3#206 (see above) was applied for the 'intrinsic' FE, assuming $\beta_{geo} = 2$ and $S_{geo} = 1 \cdot 10^{-10}$ cm². The curve fits the data points very well, if we consider a certain deviation from the assumed geometric values for each site. Also the changes of the averaged FN parameters of each sample due to the different treatments take place along this curve or, in case of PK9, along a similar curve. Therefore, theoretical models are required to explain the empirical formula.

## 4. CONCLUSION

In our recent experiments it was shown that the 'parasitic' FE observed on broad area Nb cathodes after wet surface preparation and HT can be ascribed to the geometric field enhancement of conducting particles. For this one has to take into account that both the coarse shape and the microstructure of the particles lead to a superimposed geometric field enhancement. Furthermore the 'parasitic' FE is influenced by adsorbates and surface compounds. A strong variation of $S_{FN}$, unrealistically high $S_{FN}$, and finally a correlation between the parameters $\beta_{FN}$ and $S_{FN}$, which are in principle independent, was observed. By means of experimental data we have obtained an empirical description of the changes in the FN parameters due to adsorption and desorption. These results confirms our assumption that the $\beta_{FN}$-$S_{FN}$-correlation is mainly determined by adsorbates.
Local measurement of the 'intrinsic' FE on four broad area Nb cathodes after different surface treatments showed a good agreement with the FN theory. Similar to the findings at the 'parasitic' emitters an additional influence of adsorbates was detected, leading also to a $\beta_{FN}$-$S_{FN}$-correlation, strong $S_{FN}$-variation, and unrealistically high $S_{FN}$. The $\beta_{FN}$-$S_{FN}$-variations were in correspondence with our empirical description of the adsorbate influence. The 'natural' $Nb_2O_5$-layer was found to result in enhanced $\beta_{FN}$ and lowered $S_{FN}$. The presence of this layer causes, of course, different electronic conditions (e.g. work function) as well as slightly changed surface roughness of the Nb by the oxide formation.
At emitting particles a deactivation of the FE was observed due to UHV heating at temperatures above 1200°C. The results suggest melting or evaporation of particles, phase transitions, or smoothening of micro/nano-protrusions to be responsible for this process. In contrast, activation of particles was detected after HT's between 200°C to 800°C. The possibility that certain phases of niobium carbides or niobium sulfides enhance the intrinsic emission on field enhancing particles, could be ruled out. Several observations suggest an activation depending on the conductivity of the particles or on the contact between conducting particles and cathode. In the framework of this idea the decreasing oxide layer or phase transitions in particle or contact could be crucial. For the activation after prior 1400°C HT, however, this mechanism has as a pre-condition that even after the high temperature treatment there is still e.g. an insulating (oxide) layer left between some particles and the cathode. Furthermore, after getting the required electrical contact by high temperature HT the deactivation has to take place immediately. The proposed mechanism for the activation is supported by the finding that prior long-term HT ($\approx$ 3 h) at 1400°C lessens the ability for a renewed activation.

### Acknowledgments

We wish to thank P. Kneisel and D. Reschke for their cooperation in the sample preparation. The financial support of the DESY, especially for purchasing the ion gun, is gratefully acknowledged. This work was funded in part by the Federal Minister for Research and Technology under the contract number 057WT80P7.

### References

[1] see e.g. Proc. of the 7th Workshop on RF Superconductivity, ed. by B. Bonin, CE Saclay, Gif sur Yvette, France (1995), and of this Workshop.
[2] N. Pupeter, E. Mahner, A. Matheisen, G. Müller, H. Piel, D. Proch, Proc. of the 4th Eur. Particle Acc. Conf., Vol. 3, ed. by V. Suller and Ch. Petit-Jean-Genaz, London, 2066 (1994).
[3] I. Brodie, J. Appl. Phys. 35, 2324 (1964).

[4] B. M. Cox, J. Phys. D: Appl. Phys. 8, 2065 (1975).
[5] K. H. Bayliss, R. V. Latham, Proc. Roy. Soc. London A 403, 285 (1986).
[6] N. S. Xu, R. V. Latham, J. Phys. D: Appl. Phys. 19, 477 (1986).
[7] M. Jimenez, R. J. Noer, G. Jouve, J. Jodet, B. Bonin, J. Phys. D: Appl. Phys. 27, 1038 (1994).
[8] T. Habermann, A. Göhl, G. Müller, N. Pupeter, H. Piel, Proc. of the 5th Eur. Particle Acc. Conf., Vol. 3, ed. by S. Myers, A. Pacheco, R. Pascual, Ch. Petit-Jean-Genaz, J. Poole, Barcelona, Spain, 2082 (1996).
[9] N. Pupeter, Ph.D. thesis, WUB-DIS 96-16, University of Wuppertal (1996).
[10] J. Halbritter, Appl. Phys. A 43, 1 (1987).
[11] M. Jimenez, R. Noer, G. Jouve, C. Antoine, J. Jodet, B. Bonin, J. Phys. D: Appl. Phys. 26, 1503 (1993).
[12] A. Zeitoun-Fakiris, B. Juttner, J. Phys. D: Appl. Phys. 21, 960 (1988).
[13] G. Ehrlich, T. W. Hickmott, F. G. Hudda, J. Chem. Phys. 28, 506 (1985).
[14] C. B. Duke, M. E. Alferieff, J. Chem. Phys. 46, 923 (1967).
[15] E. Mahner, N. Minatti, H. Piel, N. Pupeter, Appl. Surf. Sci. 67, 23 (1993).
[16] E. Mahner, Ph.D. thesis, WUB-DIS 95-7, University of Wuppertal (1995).
[17] N. Pupeter, A. Göhl, T. Habermann, A. Kirschner, E. Mahner, G. Müller, H. Piel, Particle Accelerators 53, 77 (1996).
[18] E. Mahner, Particle Accelerators 46, 67 (1994).
[19] Ph. Niedermann, N. Sankarraman, R. J. Noer, Ø. Fischer, J. Appl. Phys. 59, 892 (1986).
[20] E. Fromm, E. Gebhardt, Gase und Kohlenstoff in Metallen, Springer, Berlin (1976).
[21] A. N. Zelikman, Yu. D. Chistyakov, G. V. Indenbaum, O. R. Krein, Sov. Phys. Crysallogr. 6, 308 (1961).
[22] R. J. Noer, Ph. Niedermann, N. Sankarramann, Ø. Fischer, J. Appl. Phys. 59, 3851 (1986).
[23] W. Ermrich, A. van Oostrom, Solid State Communications 5, 471 (1967).
[24] M. Bartsch, Computer Phys. Comm. 72, 22 (1992).
[25] H. E. Clark, R. D. Young, Surf. Sci. 12, 385 (1968).